WAVELET-BASED RECONSTRUCTION FOR UNLIMITED SAMPLING

Sunil Rudresh, Aniruddha Adiga, Basty Ajay Shenoy, and Chandra Sekhar Seelamantula

Department of Electrical Engineering
Indian Institute of Science, Bangalore - 560012, India
Email: {sunilr, aaniruddha, bastys}@iisc.ac.in, chandra.sekhar@ieee.org

ABSTRACT

Self-reset analog-to-digital converters (ADCs) allow for digitization of a signal with a high dynamic range. The reset action is equivalent to a modulo operation performed on the signal. We consider the problem of recovering the original signal from the measured modulo-operated signal. In our formulation, we assume that the underlying signal is Lipschitz continuous. The modulo-operated signal can be expressed as the sum of the original signal and a piecewise-constant signal that captures the transitions. The reconstruction requires estimating the piecewise-constant signal. We rely on local smoothness of the modulo-operated signal and employ wavelets with sufficient vanishing moments to suppress the polynomial component. We employ Daubechies wavelets, which are most compact for a given number of vanishing moments. The wavelet filtering provides a sequence consisting of a sum of scaled and shifted versions of a kernel derived from the wavelet filter. The transition locations are estimated from the sequence using a sparse recovery technique. We derive a sufficient condition on the sampling frequency for ensuring perfect reconstruction of the smooth signal. We validate our reconstruction technique on a signal consisting of sinusoids in both clean and noisy conditions and compare the reconstruction quality with the recently developed repeated finite-difference method.

Index Terms— Wavelets, unlimited sampling, self-reset ADC, vanishing moments, sparse recovery.

1. INTRODUCTION

The standard process of digitizing a signal involves bandlimiting it by passing it through an anti-aliasing filter and then sampling using an analog-to-digital converter (ADC). The sampling rate is determined by the well known Shannon-Nyquist theorem, according to which a bandlimited signal can be reconstructed exactly by taking the measurements of the signal at the rate which is at least twice the signal's bandwidth [1]. The signals that we encounter in real world are not bandlimited and have a wide dynamic range. In practice, ADCs have a finite dynamic range $[-\lambda, \lambda]$, and when the input signal exceeds this range, the signal gets clipped (cf. Fig. 1). Henceforth, we refer to these ADCs as clipping-ADCs (C-ADCs). The problem of restoring the signal from its clipped version is a frequently encountered problem [2–5]. Typically, the restoration methods nearly mitigate the effect of clipping at the expense of oversampling. The advancement of complementary metal oxide semiconductor (CMOS) technology has enabled one to build a large variety of solutions for widening the dynamic range of CMOS image sensors (cf. [6–8] and references therein).

The authors would like to thank the Science and Engineering Research Board (SERB), Government of India for funding this work through the project "Sub-Nyquist Sampling."

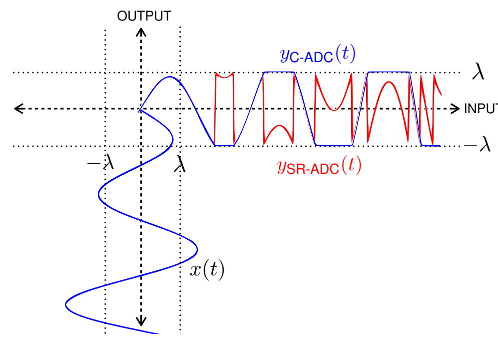

Fig. 1. An illustration of the transfer characteristics of a clipping-ADC and a self-reset-ADC with the thresholds at $\pm\lambda$.

Another class of ADCs that has been developed employ a reset technique every time the input signal goes beyond the dynamic range of the ADC. These ADCs are called *folding ADCs* [9] or self-reset ADCs (SR-ADCs) [10, 11]. When the signal reaches the upper (lower) threshold point, it folds back by a factor of 2λ and starts at the lower (upper) threshold. This phenomenon is equivalent to applying a modulo operation on the input signal. The acquisition technique aids in handling signals with high dynamic range. Most of the CMOS SR-ADCs are developed for image acquisition with pixel-level reset ability, and have found applications in brain imaging [12]. The transfer characteristics of an SR-ADC vis-à-vis the C-ADC, with saturation thresholds at λ and $-\lambda$ are illustrated in Fig. 1. If the input signal $x(t)$ has a high dynamic range, which exceeds the saturation thresholds, the output of a C-ADC, $y_{\text{C-ADC}}(t)$ (blue) is a clipped version of $x(t)$ while the output of a SR-ADC, $y_{\text{SR-ADC}}(t)$ (red) has fold-back, which captures all the variations in the input signal. Mathematically, the output $y(t)$ of the SR-ADC is represented as a modulo operation performed on the input signal $x(t)$ and is given by

$$y(t) = \mathcal{M}_\lambda\{x(t)\} := \text{mod}\,(x(t) + \lambda, 2\lambda) - \lambda, \tag{1}$$

where $\lambda > 0$ is the saturation threshold. The modulo operation in (1) is defined in such a way that the output signal has the range $[-\lambda, \lambda]$. Figure 2(a) shows an input signal and its modulo-operated signal. Observe that the output signal $y(t)$ is actually the difference between $x(t)$ and a piecewise constant signal $z(t)$, that is

$$y(t) = x(t) - z(t), \tag{2}$$

$$z(t) = \sum_k \alpha_k \mathbf{1}_{[t_k, t_{k+1}]}(t), \tag{3}$$

where $z(t)$ takes the values that are integer multiples of 2λ, that is $\text{range}(z) \in 2\lambda\mathbb{Z}$, $\mathbf{1}_{[t_1,t_2]}$ is the indicator function on $[t_1, t_2]$, and $\{t_k\}_{k\in\mathbb{Z}}$ denotes the folding instants with $t_k > t_{k-1}, \forall k$. Figure 2(b) shows the signal $z(t)$ corresponding to the signal $x(t)$ in Fig. 2(a). Now, along with $y(t)$, the parameters $\{t_k, \alpha_k\}_{k\in\mathbb{Z}}$ completely determine the signal. Also, it is to be noted that $\alpha_{k+1} = \alpha_k \pm 2\lambda$ based on whether the k^{th} transition is positive or negative, that is, whether $x(t_k^+)$ is greater than or less than $x(t_k^-)$, respectively. In practice, we have access to the samples of $y(t)$ that are obtained at the intervals of T. The discrete counterparts of (2) and (3) are given as

$$\begin{aligned} y(nT) &= x(nT) - z(nT), \\ z(nT) &= \sum_k \alpha_k \mathbf{1}_{[\![n_k, n_{k+1}]\!]}(nT), \end{aligned} \tag{4}$$

where $y(nT) = \mathcal{M}_\lambda\{x(nT)\}$, and $\{n_k\}_{k\in\mathbb{Z}} \in T\mathbb{Z}$ denotes the folding instants with $n_k > n_{k-1}, \forall k$. In this context, we seek to recover $\{x(nT)\}$ from the measurements $\{y(nT)\}$.

Over the past six decades, Shannon's sampling theory has been extended to a wider class of signals that are not necessarily bandlimited such as signals in shift-invariant spaces [13], union of subspaces [14,15], multi band signals [16–18], finite-rate-of-innovation signals [19,20], etc.. Although hardware development of SR-ADCs has significantly improved over the past decade, the theoretical framework for sampling and reconstruction from the samples of modulo operated signals has been relatively unexplored. The first seminal contribution in this direction was made recently by Bhandari et al. [21], who also effectively introduced the problem to the signal processing community and developed the first algorithm with provable reconstruction guarantees. The key idea proposed by them leverages on the fact that the N^{th}-order finite difference of a sequence $x(nT)$ obtained by sampling a bandlimited signal $x(t)$ is bounded from above and N can be chosen such that $\|\Delta^N x\|_\infty < \lambda$, where the first-order finite-difference is defined as $\Delta x(n) = x((n+1)T) - x(nT)$. They also provided sufficient conditions on the sampling rate for guaranteed reconstruction of $x(nT)$ from $y(nT)$. Henceforth, we refer to this method as repeated finite-difference (RFD) method, which also forms the benchmark for performance comparison.

1.1. This Paper

In this paper, we address both the continuous-domain problem:

$$\text{Given } y(t) = \mathcal{M}_\lambda\{x(t)\}, \text{ reconstruct } x(t), \tag{5}$$

and its discrete-domain counterpart:

$$\text{Given } y(nT) = \mathcal{M}_\lambda\{x(nT)\}, \text{ reconstruct } x(nT). \tag{6}$$

In Section 2, we consider the continuous domain problem where we employ properties of wavelets to annihilate polynomials and estimate the piecewise smooth signal $z(t)$ given by (3).

The discrete-domain counterpart (Section 3) requires the property of annihilation of discrete polynomials for wavelet filters. Employing the Daubechies wavelet of order p, we present conditions on the sampling interval to guarantee reconstruction in the context of Lipschitz continuous signals. The methodology involves wavelet filtering and computing the folding instants n_k in (4). The problem of reconstruction of the folding instants is shown to be equivalent to a sparse recovery problem in an appropriate basis, which is solved using the LASSO formulation. Unlike the phase unwrapping problem, where one has access to continuous wrapped phase, in problem (6), we have access to the discrete version of the wrapped signal.

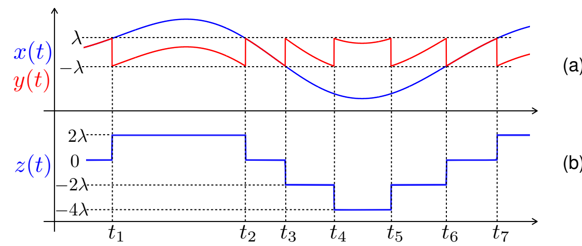

Fig. 2. Modulo operation: (a) Input signal $x(t)$ (in blue) and its modulo version $y(t)$ (in red); and (b) piecewise-constant signal $z(t)$.

In order to validate the theoretical developments, we present simulation results demonstrating reconstruction of a signal from its modulo measurements (Section 4). We consider both noise-free and noisy measurement scenarios, and carry out the proposed reconstruction. Further, we compare our results with that of RFD method for various signal-to-noise ratios (SNRs).

2. CONTINUOUS-DOMAIN ANALYSIS

In this section, we address (5) where we assume suitable regularity conditions on $x(t)$. In view of (2), it suffices to determine $z(t)$, which, in turn, is characterized by the parameters $\{t_k, \alpha_k\}_{k\in\mathbb{Z}}$ given by the representation in (3). Thus, the problem (5) is now reduced to computing $\{t_k, \alpha_k\}_{k\in\mathbb{Z}}$ from $y(t)$.

Our approach relies on annihilating a polynomial of degree p, for which we employ a wavelet. In this context, we recall the following definition for vanishing moments of a wavelet. The notation $[\![0, p]\!]$ indicates the set of integers from 0 to p.

Definition 1 (Vanishing moments)**.** *A wavelet ψ has $p+1$ vanishing moments if $\int t^k \psi(t)\,\mathrm{d}t = 0$, for $k \in [\![0, p]\!]$.*

If $x(t)$ is a polynomial of degree p, then a wavelet ψ that has $p+1$ vanishing moments annihilates it, that is,

$$(x * \psi)(t) = 0, \tag{7}$$

for all $t \in \mathbb{R}$. We employ (7) to locate the folding instants $\{t_k\}$. The convolution of $y(t)$ with $\psi(t)$ provides us with a sum of time-shifted versions of a kernel $\xi(t)$ derived from the wavelet $\psi(t)$, as detailed in the following lemma.

Lemma 1. *Let $x(t)$ be a polynomial of degree p, $\psi(t)$ be a wavelet with $p+1$ vanishing moments, and $y(t) = \mathcal{M}_\lambda\{x(t)\}$. Then, we have,*

$$y_\psi(t) := (y * \psi)(t) = \sum_k (\alpha_k - \alpha_{k-1})\xi(t - t_k), \tag{8}$$

where $\xi(t) = -\int_{-\infty}^{t} \psi(\tau)\,\mathrm{d}\tau$, and α_ks are as defined in (3).

Proof. In view of (2), the convolution of $y(t)$ with $\psi(t)$ yields

$$y_\psi(t) = (x * \psi)(t) - (z * \psi)(t) = -(z * \psi)(t), \tag{9}$$

where the second equality follows from (7).

Since $z(t)$ has a representation given by (3), we have

$$
\begin{aligned}
-(z*\psi)(t) &= -\left(\sum_k \alpha_k \mathbf{1}_{[t_k,t_{k+1}]} * \psi\right)(t),\\
&= -\sum_k \alpha_k(\psi * (u_{t_k} - u_{t_{k+1}}))(t),\\
&= -\sum_k (\alpha_k - \alpha_{k-1})(\psi * u_{t_k})(t),\\
&= \sum_k (\alpha_k - \alpha_{k-1})\xi(t - t_k),
\end{aligned}
$$

and the result follows. □

From Lemma 1 and (2), we see that reconstructing $x(t)$ from $y(t)$ is achieved by computing the folding instants t_ks and the weights $\alpha_k - \alpha_{k-1}$ from $y_\psi(t)$ as given by (8). Since $y_\psi(t)$ is a sum of time-shifted and scaled versions of $\xi(t)$, the α_ks can be estimated, for instance, by using a matched filter with the known kernel $\xi(t)$. Since the support of $\xi(t)$ is restricted to lie in the interval $[0, 2p-1]$, exact reconstruction is possible whenever $(t_k - t_{k-1}) > 2p-1, \forall k$. This is satisfied for Lipschitz-continuous functions if $\frac{2\lambda}{L} > (2p-1)$. This bound is sufficient, but is actually overly conservative. The above analysis can be extended to smooth signals that can be approximated by polynomials by using a truncated Taylor series expansion [23, Ch. 6].

3. DISCRETE DOMAIN

For digital implementation, we need to take into account that working with samples of $x(t)$ and $\psi(t)$ may not lead to the desired annihilation property given by (7). If either $\psi(t)$ or $x(t)$ is not bandlimited, then convolving and sampling operations do not commute. Thus, while addressing problem (6), we need to understand the effect of the sampling interval T. We employ the square bracket notation: $x[n] := x(nT)$, and $y[n] := y(nT)$.

3.1. Polynomial Annihilation

To obtain the discrete counterpart of (7), we need to consider annihilation of the sampled polynomial of degree p. Towards this end, we need to construct a filter $g(n)$ such that

$$
\sum_{n\in\mathbb{Z}} n^k g[n] = 0, \text{ for every } k \in [\![0,p]\!]. \tag{10}
$$

These conditions yield the Daubechies wavelet filter of order p [22, 23], with support $[\![0, 2p-1]\!]$, which is the least among all wavelet filters that annihilate polynomials of degree p. Thus, (10) serves as the discrete counterpart to (7) with the role of the wavelet $\psi(t)$ replaced by the filter $g[n]$. Analogous to the continuous-domain annihilation (9), if $x[n] := x(nT)$ are the samples of a polynomial $x(t)$ of degree p, we have $(y*g)[n] = (x*g)[n] - (z*g)[n] = -(z*g)[n]$, where the second equality is a consequence of (10). The discrete counterpart of Lemma 1 is provided next.

Lemma 2. *Let $x[n]$ be the samples of a polynomial of degree p, and let $g[n]$ be a discrete wavelet filter with $p+1$ vanishing moments. Then, we have, with $m[n] := -\sum_{k=-\infty}^{n} g[k]$, that*

$$
y_g[n] := (y*g)[n] = \sum_k (\alpha_k - \alpha_{k-1})\, m[n - n_k]. \tag{11}
$$

Algorithm 1 : WAVElet-Based Unlimited Sampling (WAVE-BUS).

- Input: $y(nT) = \mathcal{M}_\lambda\{x(nT)\}$, L, λ, p, T
- Output: $\bar{x}(nT)$
- Method:
  1. Wavelet filtering: $(y_g)[n] = (y*g)[n]$
  2. LASSO (13) (compute n_ks and α_ks): $\arg\min_h \|Ah - y_g\|_2 + \gamma\|y_g\|_1$
  3. Compute $\bar{z}[n] : \sum_k \alpha_k \mathbf{1}_{[\![n_k,n_{k+1}]\!]}$
  4. Reconstruct $x[n] : \bar{x}[n] = y[n] + \bar{z}[n]$

The proof is straightforward and follows along the lines of Lemma 1 with the role of ψ replaced by g. The reconstruction of $x[n]$ from $y[n]$ now requires us to compute the discrete folding instants n_ks and α_ks from (11), which is a sum of scaled and shifted versions of $m[n]$.

3.2. Computing the Discrete Folding Instants

Defining $\beta_k = \alpha_k - \alpha_{k-1}$, we rewrite (11) as

$$
y_g[n] := \sum_k \beta_k m[n - n_k]. \tag{12}
$$

Expressing the above equation in matrix form gives $y_g = Ah$, where A is the convolutional dictionary of all integer-time shifted versions of $m[n]$ and h is a sparse vector whose support is precisely $\{n_k\}$ with $h(n_k) = \beta_k$. The cardinality of $\{n_k\}$, which is equal to the number of times the signal $x(t)$ folds back, is much less than the length of the signal if the sampling rate is sufficiently high and $x(t)$ is sufficiently regular, as discussed below. It now remains to compute n_ks and β_k from the sparse representation. While several methods exist for sparse reconstruction, we employ LASSO [24]:

$$
\min_h = \|y_g - Ah\|_2 + \gamma\|h\|_1, \tag{13}
$$

where γ is the regularization parameter that enhances sparsity. Once the parameters $\{n_k, \beta_k\}$ are computed, we determine $\{\alpha_k\}$ and construct $z[n]$ as dictated by (4), from which $x[n]$ can be obtained.

The performance of LASSO depends on the values that n_k take and the support of $m[n]$, which is equal to the support of $g[n]$. We see that if $\min_k (n_k - n_{k-1}) > \text{supp}\{m[n]\}$, then no two shifted versions of $m[n]$ overlap thereby ensuring perfect reconstruction. However, empirically it is seen that, even in case of an overlap of about one-half to two-thirds of the support, LASSO reconstructs the parameters with a high degree of accuracy. We next develop a sampling scheme that ensures no overlap between successive shifts of $m[n]$ in (12). Define

$$
T_f := \min_k (n_k - n_{k-1})
$$

to be the minimum folding interval. Since the length of the support of the Daubechies wavelet filter is $2p$, we see that a sampling interval

$$
T \le \frac{T_f}{2p} \tag{14}
$$

is sufficient to ensure that there is no overlap. While evaluating T_f is not practical, we have the following lower bound on T_f whenever the underlying signal $x(t)$ is Lipschitz continuous.

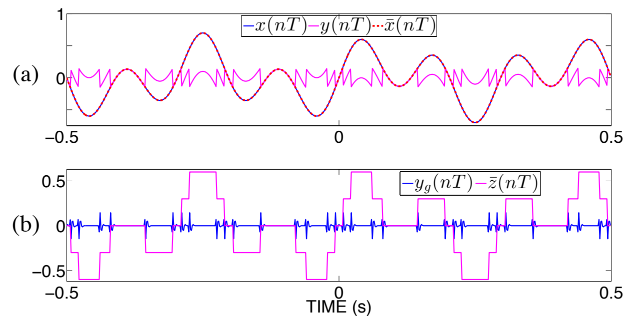

Fig. 3. WAVE-BUS with $\lambda = 0.15$: (a) Signal $x(nT)$, its modulo samples $y(nT)$, and the reconstruction $\bar{x}(nT)$; (b) wavelet filter output $y_g(nT)$, and the estimate $\bar{z}(nT)$. The reconstruction error was computed to be -330 dB.

Lemma 3. *Let $x(t)$ be a Lipschitz continuous signal that satisfies $|x(a) - x(b)| \leq L|b - a|$ and $y(t) = \mathcal{M}_\lambda\{x(t)\}$. Then, we have $\tilde{T}_f := \frac{2\lambda}{L} \leq T_f$.*

Proof. From the defining property of Lipschitz continuity, we have

$$|x(t + \tilde{T}_f) - x(t)| \leq L\tilde{T}_f < 2\lambda, \text{ for all } t,$$

and hence, starting at any t_k, no folding happens in the interval $(t_k, t_k + \tilde{T}_f)$. Thus $\tilde{T}_f \leq T_f$. □

From Lemma 3 and (14), the following condition

$$T \leq \frac{2\lambda}{L(2p)} \tag{15}$$

ensures that (14) is satisfied. This sampling interval is practically realizable whenever the Lipschitz constant is known. The sampling rate f is then given by $f = \frac{1}{T} \geq \frac{Lp}{\lambda}$. The proposed technique to reconstruct $x(t)$ from $y(t)$ is referred as *WAVElet-Based Unlimited Sampling* (WAVE-BUS) and is presented in Algorithm 1.

4. SIMULATION RESULTS

We show simulation results of the proposed WAVE-BUS first in the noiseless case and then consider the noisy scenario. Also, we demonstrate improved reconstruction performance in the presence of noise over the RFD method. We consider a signal, which is a linear combination of two sinusoids of amplitude 0.7 and 0.5, and frequencies 7 Hz and 4 Hz. The parameter λ is set to 0.15 and the sampling interval as per the sufficiency condition stated in (15) is $T < 0.43$ ms. While the Nyquist rate provides the minimum sampling rate required to reconstruct a bandlimited signal from its samples, it ceases to apply when we seek to reconstruct the signal from its modulo version owing to the discontinuities. As the bound on T is conservative, we choose $T = 2$ ms and Daubechies wavelet filter of order 4 to validate the proposed reconstruction method in all our simulations and, for a fair comparison, the sampling interval and other parameters are chosen such that the sufficiency conditions of the RFD method are met. The signal, its modulo samples, reconstructed signal ($\bar{x}[n]$), and the estimate $\bar{z}(nT)$ are shown in Fig. 3.

Next, we consider the scenario wherein the modulo samples $\{y[n]\}$ are corrupted by noise as $\tilde{y}[n] = y[n] + w[n]$, where $\{w[n]\}$ is zero mean, additive, white Gaussian noise with variance σ^2. The input SNR is defined as $\text{SNR}_{\text{in}} = 10\log_{10}\frac{\|y[n]\|_2^2}{\sigma^2}$ dB and the signal-to-reconstruction noise ratio (SRNR) $:= 10\log_{10}\frac{\sum_n |x[n]|^2}{\sum_n |x[n] - \bar{x}[n]|^2}$ dB is computed over L independent noise realizations. Figure 4 shows the reconstruction performance of WAVE-BUS and RFD methods at $\text{SNR}_{\text{in}} = 20$ dB. The SRNR for various SNR_{in} for $L = 300$ is shown in Fig. 5. We observe the robustness of the proposed reconstruction method in the presence of noise as indicated by the plots. The superior reconstruction of the WAVE-BUS method is attributed to the fact that there is no accumulation of noise as in the case of the RFD method.

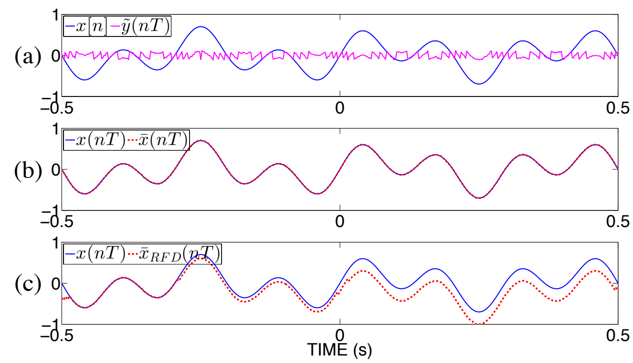

Fig. 4. Unlimited sampling in the presence of noise ($\text{SNR}_{\text{in}} = 20$ dB and $\lambda = 0.05$): (a) The signal $x(nT)$ and its noisy modulo samples $\tilde{y}(nT)$. Reconstructions using (b) WAVE-BUS and (c) RFD methods with reconstruction errors at -80 dB and -7 dB, respectively.

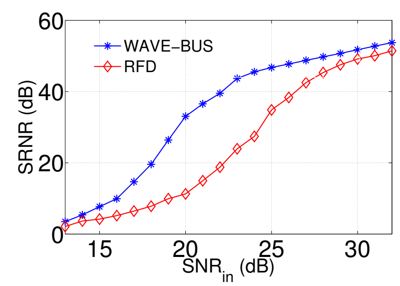

Fig. 5. SRNR for WAVE-BUS and RFD methods versus SNR_{in}.

5. CONCLUSIONS

We considered the problem of unlimited sampling and developed a wavelet-based scheme to reconstruct from modulo measurements. We provided sufficient conditions on the sampling interval for perfect reconstruction of smooth signals in both continuous- and discrete-time domains. The sufficiency conditions are given in terms of the threshold of the ADC and Lipschitz constant of the smooth signal. We demonstrated the performance of the reconstruction method both in noiseless and noisy signal scenarios. One of the merits of the proposed method is the superior noise robustness over the repeated finite-difference method. Further, the proposed WAVE-BUS method is applicable to smooth signals in general and not restricted to bandlimited signals. For the discrete version, we recovered the folding instants by employing LASSO. In principle, any sparse recovery technique could be employed and the sampling rate could be further reduced, limited only by the ability of the technique to super-resolve.

6. REFERENCES

[1] C. E. Shannon, "A mathematical theory of communication," *The Bell Systems Technical Journal*, vol. 27, pp. 623–656, 1948.

[2] J. S. Abel and J. O. Smith, "Restoring a clipped signal," in *Proceedings of International Conference on Acoustics, Speech, and Signal Processing (ICASSP)*, Apr 1991, pp. 1745–1748 vol.3.

[3] Z. Kollár, J. Gazda, P. Horváth, L. Varga, and D. Kocur, "Iterative signal reconstruction of deliberately clipped SMT signals," *Science China Information Sciences*, vol. 57, no. 2, pp. 1–13, Feb 2014.

[4] H. Saeedi, M. Sharif, and F. Marvasti, "Clipping noise cancellation in OFDM systems using oversampled signal reconstruction," *IEEE Communications Letters*, vol. 6, no. 2, pp. 73–75, Feb 2002.

[5] U. K. Kwon, D. Kim, and G. H. Im, "Amplitude clipping and iterative reconstruction of MIMO-OFDM signals with optimum equalization," *IEEE Transactions on Wireless Communications*, vol. 8, no. 1, pp. 268–277, Jan 2009.

[6] G. Wetzstein, I. Ihrke, and W. Heidrich, "Sensor saturation in Fourier multiplexed imaging," in *Conference on Computer Vision and Pattern Recognition (CVPR)*. IEEE, 2010, pp. 545–552.

[7] J. Rhee and Y. Joo, "Wide dynamic range CMOS image sensor with pixel level ADC," *Electronics Letters*, vol. 39, no. 4, pp. 360–361, Feb 2003.

[8] A. Spivak, A. Belenky, A. Fish, and O. Yadid-Pecht, "Wide-dynamic-range CMOS image sensors: Comparative performance analysis," *IEEE Transactions on Electron Devices*, vol. 56, no. 11, pp. 2446–2461, Nov 2009.

[9] W. Kester, "ADC architectures VI: Folding ADCs (MT-025 tutorial)," *Analog Devices, Technical Report*, vol. 27, pp. 623–656, 2009.

[10] D. Park, J. Rhee, and Y. Joo, "A wide dynamic-range CMOS image sensor using self-reset technique," *IEEE Electron Device Letters*, vol. 28, no. 10, pp. 890–892, Oct 2007.

[11] D. Park, Y. Joo, and S. Koppa, "A simple and robust self-reset CMOS image sensor," in *IEEE International Midwest Symposium on Circuits and Systems*, Aug 2010, pp. 680–683.

[12] K. Sasagawa, T. Yamaguchi, M. Haruta, Y. Sunaga, H. Takehara, H. Takehara, T. Noda, T. Tokuda, and J. Ohta, "An implantable CMOS image sensor with self-reset pixels for functional brain imaging," *IEEE Transactions on Electron Devices*, vol. 63, no. 1, pp. 215–222, Jan 2016.

[13] M. Unser, "Sampling-50 years after Shannon," *Proceedings of the IEEE*, vol. 88, no. 4, pp. 569–587, April 2000.

[14] M. Mishali, Y. C. Eldar, and A. J. Elron, "Xampling: Signal acquisition and processing in union of subspaces," *IEEE Transactions on Signal Processing*, vol. 59, no. 10, pp. 4719–4734, Oct. 2011.

[15] K. Gedalyahu and Y. C. Eldar, "Time-delay estimation from low-rate samples: A union of subspaces approach," *IEEE Transactions on Signal Processing*, vol. 58, no. 6, pp. 3017–3031, June 2010.

[16] M. Mishali and Y. C. Eldar, "Blind multiband signal reconstruction: Compressed sensing for analog signals," *IEEE Transactions on Signal Processing*, vol. 57, no. 3, pp. 993–1009, Mar. 2009.

[17] R. Venkataramani and Y. Bresler, "Optimal sub-Nyquist nonuniform sampling and reconstruction for multiband signals," *IEEE Transactions on Signal Processing*, vol. 49, no. 10, pp. 2301–2313, Oct 2001.

[18] P. Feng and Y. Bresler, "Spectrum-blind minimum-rate sampling and reconstruction of multiband signals," in *Proceedings of International Conference on Acoustics, Speech, and Signal Processing (ICASSP)*, May 1996, vol. 3, pp. 1688–1691 vol. 3.

[19] M. Vetterli, P. Marziliano, and T. Blu, "Sampling signals with finite rate of innovation," *IEEE Transactions on Signal Processing*, vol. 50, no. 6, pp. 1417–1428, Jun. 2002.

[20] T. Blu, P. L. Dragotti, M. Vetterli, P. Marziliano, and L. Coulot, "Sparse sampling of signal innovations," *IEEE Signal Processing Magazine*, vol. 25, no. 2, pp. 31–40, Mar. 2008.

[21] A. Bhandari, F. Krahmer, and R. Raskar, "On unlimited sampling," in *Proceedings of International Conference on Sampling Theory and Applications (SampTA)*, July 2017, pp. 31–35.

[22] I. Daubechies, *Ten Lectures on Wavelets*, SIAM, 1992.

[23] S. Mallat, *A Wavelet Tour of Signal Processing, Third Edition: The Sparse Way*, Academic Press, 3 edition, 2008.

[24] R. Tibshirani, "Regression shrinkage and selection via the lasso," *Journal of the Royal Statistical Society, Series B*, vol. 58, pp. 267–288, 1994.